Asymmetric quantum dot in a microcavity as a nonlinear optical element

I. G. Savenko,[1] O. V. Kibis,[2] and I. A. Shelykh[1,3]

[1]*Science Institute, University of Iceland, Dunhagi 3, IS-107, Reykjavik, Iceland*

[2]*Department of Applied and Theoretical Physics, Novosibirsk State Technical University, Karl Marx Avenue 20, 630092 Novosibirsk, Russia*

[3]*Division of Physics and Applied Physics, Nanyang Technological University 637371, Singapore*

(Received 16 March 2012; published 15 May 2012)

We have investigated theoretically the interaction between individual quantum dot with broken inversion symmetry and an electromagnetic field of a single-mode quantum microcavity. It is shown that in the strong-coupling regime the system demonstrates nonlinear optical properties and can serve as emitter of the terahertz radiation at Rabi frequency of the system. Analytical results for the simplest physical situations are obtained and a numerical quantum approach for calculating an emission spectrum is developed.

DOI: 10.1103/PhysRevA.85.053818 PACS number(s): 42.50.Pq, 78.67.Hc, 42.79.Gn

I. INTRODUCTION

Quantum microcavities provide a unique laboratory for studies of strong light-matter coupling. First observed two decades ago [1], the strong-coupling regime is now routinely achieved in different kinds of microcavities [2]. From the fundamental viewpoint, it is interesting as a basis to investigate various collective phenomena in condensed-matter systems such as Bose-Einstein condensation (BEC) [3] and superfluidity [4]. From the viewpoint of applications, it opens a way to the realization of optoelectonic devices of the new generation [5]: room-temperature polariton lasers [6], polarization-controlled optical gates [7], and others.

Several applications of the strong-coupling regime were also proposed for quantum information processing [8–10]. In this case, one should be able to tune the number of emitted photons in controllable way. This is hard to achieve in planar microcavities where the number of elementary excitations is macroscopically large but is possible in microcavities containing single quantum dots (QDs), where QD exciton can be coupled to a confined electromagnetic mode provided by a micropillar (etched planar cavity) [11], a defect of the photonic crystal [12], or a whispering gallery mode [13].

Depending on the size of the QD, its elementary excitations can behave as fermions (small QDs whose size is comparable with exciton radius in the bulk material) [14], bosons (large QDs whose size is much larger than exciton radius in the bulk material) [15], or particles with intermediate statistics (medium size QDs) [16]. In the current paper, we consider a small single QD in a microcavity that corresponds to the case of fermions. For symmetric QDs such system can be described by the well-known Jaynes-Cummings Hamiltonian [17], which predicts transformation of the Rabi doublet to the Mollow triplet in the emission spectrum as intensity of the external pump growth for both coherent [18] and incoherent excitation schemes [19]. On the other hand, incorporation of the asymmetry into the quantum system can radically change its emission pattern and lead to the opening of optical transitions which were forbidden in the symmetric case. In particular, the breaking of inversion symmetry opens optical transitions at the Rabi frequency at QDs placed in a strong external laser field [20]. A similar effect occurs for asymmetric quantum wells placed inside a planar microcavity [21,22]. In this paper we consider a modification of the emission spectrum of asymmetric QDs inside a single-mode microcavity using a fully quantum approach.

The paper is organized as follows. In Sec. II we describe the formalism and introduce the model Hamiltonian. In Sec. III we obtain analytical solutions for important particular cases. In Sec. IV we discuss the incorporation of pump and decay terms into the Hamiltonian and present numerical calculations of the emission spectrum. Section V contains discussions and conclusions.

II. MODEL

We model the QD as a two-level quantum system with the ground state $|g\rangle$ and excited state $|e\rangle$ with energies ε_g and ε_e, respectively. The QD is placed inside a cavity and interacts resonantly with confined electromagnetic mode of the frequency ω_c (Fig. 1). Since an electromagnetic field can transfer an electron in the QD from the valence band into the conduction band, the ground state $|g\rangle$ corresponds to the absence of free carriers while the first excited state $|e\rangle$ is the state with an electron in the conduction band and a hole in the valence band. Therefore, the energy difference $\Delta = \varepsilon_g - \varepsilon_e$ is approximately equal to the band gap of the QD minus the excitonic correction accounting for the Coulomb attraction between the electron and the hole.

The full Hamiltonian of the system can be represented as a sum of three parts,

$$\hat{\mathcal{H}} = \hat{\mathcal{H}}_e + \hat{\mathcal{H}}_\omega + \hat{\mathcal{H}}_{\text{int}}, \tag{1}$$

where

$$\hat{\mathcal{H}}_e = \frac{\Delta}{2}\sigma_z \tag{2}$$

is the Hamiltonian of the single QD and $\sigma_{x,y,z}$ are the Pauli matrices acting in the space of the $|e\rangle$ and $|g\rangle$ states. The Hamiltonian of the free electromagnetic field reads

$$\hat{\mathcal{H}}_\omega = \hbar\omega_c a^\dagger a, \tag{3}$$

where $a, a^\dagger$ are the annihilation and creation operators for cavity photons, respectively. The Hamiltonian $\hat{\mathcal{H}}_{\text{int}}$ describes the interaction of the QD with the electromagnetic field and can be constructed as follows. The interaction of a classical

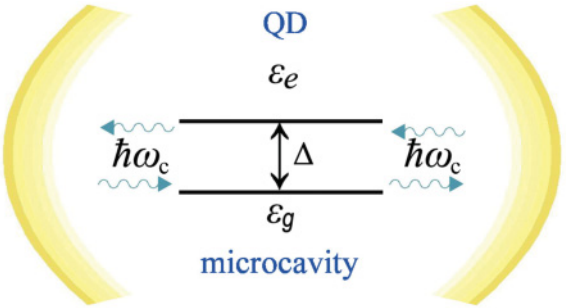

FIG. 1. (Color online) Two-level quantum dot with the band gap Δ in a single-mode microcavity with the frequency ω_c.

dipole $\mathbf{d}$ with a classical external electric field $\mathbf{E}$ is given by the expression $\hat{\mathcal{H}}_{\rm int} = -\mathbf{E}\mathbf{d}$. Within the quantum-field approach, we have to replace the classical quantities $\mathbf{d}$ and $\mathbf{E}$ with the corresponding operators,

$$\hat{\mathbf{E}} = \sqrt{\frac{\hbar\omega_c}{2\epsilon_0 V}}(\mathbf{e}a + \mathbf{e}^* a^\dagger),$$
$$\hat{\mathbf{d}} = \begin{pmatrix} \mathbf{d}_{ee} & \mathbf{d}_{eg} \\ \mathbf{d}_{ge} & \mathbf{d}_{gg} \end{pmatrix} = \frac{\mathbf{d}_{ee}+\mathbf{d}_{gg}}{2} I + \frac{\mathbf{d}_{ee}-\mathbf{d}_{gg}}{2}\sigma_z + (\mathbf{d}_{eg}\sigma^+ + \mathbf{d}_{ge}\sigma^-), \quad (4)$$

where $\mathbf{e}$ is the polarization vector of the cavity mode, ϵ_0 is the vacuum dielectric permittivity, $\mathbf{d}_{ij} = \langle i|\hat{\mathbf{d}}|j\rangle$ are dipole matrix elements of the QD, I is the unity matrix, and $\sigma^\pm = (\sigma_x \pm i\sigma_y)/2$. In the case of symmetric QD, the matrix elements $\mathbf{d}_{ee}$ and $\mathbf{d}_{gg}$ are zero. Due to the breaking of inversion symmetry in asymmetric QDs, the dipole matrix elements appear to be nonequivalent, $\mathbf{d}_{ee} \neq \mathbf{d}_{gg}$. This leads to new physical effects discussed hereafter. The interaction Hamiltonian can be written as

$$\hat{\mathcal{H}}_{\rm int} = -\hat{\mathbf{d}}\hat{\mathbf{E}} = g_R(a+a^\dagger)(\sigma^+ + \sigma^-) + g_S(a+a^\dagger)(\sigma_z + I) \approx g_R(a\sigma^+ + a^\dagger\sigma^-) + g_S(a+a^\dagger)(\sigma_z + I). \quad (5)$$

The coupling parameters $g_R = -(\mathbf{d}_{eg}\cdot\mathbf{e})\sqrt{\hbar\omega_c/2\epsilon_0 V}$ and $g_S = -(\mathbf{d}_{ee}\cdot\mathbf{e})\sqrt{\hbar\omega_c/4\epsilon_0 V}$ describe the excitation-exchange interaction and the symmetry-dependent interaction, respectively. For definiteness, we assume them to be real. The parameter V in the expressions above is the quantization volume and can be estimated as $V \approx (\lambda/2)^3$, where $\lambda = c/2\pi\omega_c$ is the characteristic wavelength corresponding to the cavity mode. We also put $\mathbf{d}_{gg} = 0$, which can be justified for nonferroelectric QDs. Indeed, asymmetry of such QDs is provided by peculiar shape and/or an external electric field. Due to this, the matrix element d_{gg} is proportional to the size of the elementary cell of the crystal lattice, while the matrix element d_{ee} is proportional to the size of the QD. As a result, in realistic QDs, one has $d_{ee} \gg d_{gg}$. To pass from the first line to the second line in Eq. (5), the rotating-wave approximation [23,24] was applied and we dropped the antiresonant terms proportional to $a^\dagger\sigma^+$ and $a\sigma^-$.

The full Hamiltonian of the system reads

$$\hat{\mathcal{H}} = \hbar\omega_c a^\dagger a + \frac{\Delta}{2}\sigma_z + g_R(a\sigma^+ + a^\dagger\sigma^-) + g_S(a+a^\dagger)(\sigma_z + I). \quad (6)$$

In the case of a symmetric QD, the coupling parameter g_S equals zero. Equation (6) then reduces to the Hamiltonian of the fully solvable Jaynes-Cummings model. Its eigenstates correspond to electronic excitations dressed by the cavity photons and can be expressed as

$$\left|\psi_n^{\pm(0)}\right\rangle = A_n^\pm|g,n\rangle + B_n^\pm|e,n-1\rangle, \quad (7)$$

where

$$A_n^\pm = \frac{\varepsilon_n^{\pm(0)} - \hbar\omega_c(n-1) - \Delta/2}{\sqrt{\left[\varepsilon_n^{\pm(0)} - \hbar\omega_c(n-1) - \Delta/2\right]^2 + g_R^2 n}}, \quad (8)$$

$$B_n^\pm = \frac{g_R\sqrt{n}}{\sqrt{\left[\varepsilon_n^{\pm(0)} - \hbar\omega_c(n-1) - \Delta/2\right]^2 + g_R^2 n}}, \quad (9)$$

and the composite electron-photon states $|g,n\rangle = |g\rangle \bigotimes |n\rangle$ and $|e,n\rangle = |e\rangle \bigotimes |n\rangle$ describe both the QD state (the ground state g or the excited state e) and the field state with n cavity photons. It should be noted that the Jaynes-Cummings Hamiltonian commutes with the excitation number operator

$$\hat{N} = a^\dagger a + (\sigma_z + I)/2, \quad (10)$$

whose eigenstates correspond to the conserved number of total electron-photon excitations in the system counted as number of the excitations in QD (zero for the state $|g\rangle$, unity for the state $|e\rangle$) plus number of the photons in the cavity mode. The eigenenergies corresponding to the states (7) are given by

$$\varepsilon_n^{\pm(0)} = \hbar\omega_c\left(n - \frac{1}{2}\right) \pm \sqrt{\frac{(\hbar\omega_c - \Delta)^2}{4} + g_R^2 n}. \quad (11)$$

In order to obtain the emission spectrum of the system, we need to analyze optical transitions between the eigenstates (7). An emitted photon goes outside the system, and a pumped photon appears in the system. Thus, there is an exchange of photons between the coupled QD-microcavity system and some external reservoir. Therefore, we can introduce the Hamiltonian of the exchange of photons between cavity and outside world,

$$\hat{\mathcal{H}}_{\rm ex} = \hbar(\Gamma^\star a r^\dagger + \Gamma a^\dagger r), \quad (12)$$

where $r^\dagger, r$ are creation and annihilation operators for the external photons and Γ is the system-reservoir coupling constant.

The probabilities (intensities) of transitions with emission of photon from the cavity are proportional to the corresponding matrix elements,

$$I_{if} \sim |\langle\psi_f, 1_R|\hat{\mathcal{H}}_{\rm ex}|\psi_i, 0_R\rangle|^2, \quad (13)$$

where the symbols ψ_f, ψ_i denote the final and initial eigenstates of the Hamiltonian (7) and 0_R and 1_R describe zero- and one-photon states of the reservoir. Substituting Eq. (12) into Eq. (13), one gets

$$I_{if} \sim |\langle\psi_f|a|\psi_i\rangle|^2 = \left(\sqrt{n_i}A_{n_f}^\pm A_{n_i}^\pm + \sqrt{n_f}B_{n_f}^\pm B_{n_i}^\pm\right)^2\delta_{n_f,n_i-1}, \quad (14)$$

where the states $|\psi_{i,f}\rangle$ are defined by Eq. (7) and integers n_i, n_f are initial and final numbers of electron-photon excitations in the system, defined earlier [see Eq. (10)].

The Kronecker δ in Eq. (14) means that only transitions changing the number of excitations by 1 are allowed in a system described by the Jaynes-Cummings Hamiltonian. It follows from Eq. (11) that in the case of resonance ($\hbar\omega_c = \Delta$) the optical spectrum contains peaks at the energies $\hbar\omega_c \pm g_R(\sqrt{n+1} \pm \sqrt{n})$, where $n = 0,1,2,\ldots$. This leads to the emission spectrum in the form of the Rabi doublet (for $n = 0$) and the Mollow triplet (for $n \gg 1$) [19]. In the intermediate regime more complicated multiplet structure can be observed [14].

It should be noted that in symmetric QDs ($g_S = 0$) transitions at the Rabi frequency $\Omega_R = 2g_R/\hbar$ are forbidden. Indeed, the transitions would occur between electron-photon states with the same number of excitations, $n_f = n_i$, which is not allowed by Eq. (14). However, these transitions become possible for asymmetric QDs, i.e., when the full Hamiltonian (6) contains the term $g_S(a + a^\dagger)(\sigma_z + 1)$ [20]. Since for realistic microcavities the frequency $\Omega_R\sqrt{n}$ lies in the terahertz (THz) range, such transitions form the physical basis for using the considered system as a tunable source of THz radiation. We will consider these transitions in more detail in the following sections.

III. ANALYTICAL SOLUTIONS

First, let us consider analytically the case of weak asymmetry. The Hamiltonian (6) then can be represented as a sum of two parts,

$$\hat{\mathcal{H}} = \hat{\mathcal{H}}_{\rm JC} + \widehat{V}, \tag{15}$$

where

$$\hat{\mathcal{H}}_{\rm JC} = \hbar\omega_c a^\dagger a + \frac{\Delta}{2}\sigma_z + g_R(a\sigma^+ + a^\dagger\sigma^-) \tag{16}$$

is the Jaynes-Cummings Hamiltonian and

$$\widehat{V} = g_S(a + a^\dagger)(\sigma_z + I) \tag{17}$$

is the term arising from the asymmetry of the QD. Considering the term (17) as a small perturbation and using the standard first-order perturbation theory, the corrected wave functions of the system can be written as

$$|\psi_n^\pm\rangle = \left|\psi_n^{\pm(0)}\right\rangle + \sum_m \sum_{\alpha=\pm} \frac{V_{nm}^{\pm\alpha}}{\varepsilon_n^{\pm(0)} - \varepsilon_m^{\alpha(0)}} \left|\psi_m^{\alpha(0)}\right\rangle, \tag{18}$$

where $|\psi_n^{\pm(0)}\rangle$ are the unperturbed eigenfunctions (7), $\varepsilon_n^{\pm(0)}$ are the corresponding eigenenergies (11), and $V_{nm}^{\pm\alpha} = \langle\psi_n^{\pm(0)}|\widehat{V}|\psi_m^{\alpha(0)}\rangle$ are the matrix elements of the perturbation (17).

It is easy to see that these matrix elements differ from zero only if $m = n \pm 1$, and, thus, states with n,$n-1$ and $n+1$ excitations become mixed by the asymmetry of the QD. This mixture leads to the opening of the optical transitions $|\psi_n^+\rangle \to |\psi_n^-\rangle$ at the frequencies $\Omega_R\sqrt{n}$. As well, transitions at double frequencies of the cavity $2\omega_c \pm \Omega_R(\sqrt{n+1} \pm \sqrt{n})/2$ become opened. The allowed transitions are shown schematically in Fig. 2.

Since the frequency $\Omega_R\sqrt{n}$ can lie in the THz range, an asymmetric QD-cavity system can be used as a nonlinear THz emitter. Using Eqs. (14) and (18), we obtain the intensity of THz transitions as follows:

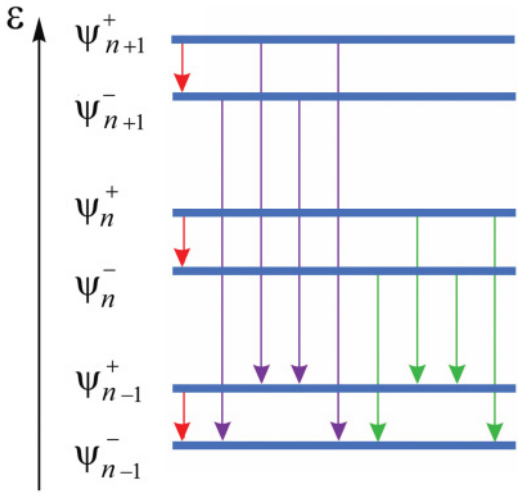

FIG. 2. (Color online) Optical transitions in the asymmetrical QD coupled with the cavity mode.

$$I_{if} \sim |\langle\psi_n^-|a|\psi_n^+\rangle|^2,$$

where

$$\langle\psi_n^-|a|\psi_n^+\rangle = \frac{V_{n-1,n}^{-+}}{\varepsilon_n^{-(0)} - \varepsilon_{n-1}^{+(0)}}(\sqrt{n}A_{n-1}^+A_n^+ + \sqrt{n-1}B_{n-1}^+B_n^+) + \frac{V_{n+1,n}^{+-}}{\varepsilon_n^{+(0)} - \varepsilon_{n+1}^{-(0)}}(\sqrt{n+1}A_n^-A_{n+1}^- + \sqrt{n}B_n^-B_{n+1}^-).$$

with coefficients $A_n^\pm$ and $B_n^\pm$ given by expressions (8) and (9), respectively.

One can also consider analytically another physical situation: The asymmetry is no longer assumed to be a weak perturbation, but photon occupation numbers are supposed to be large, $n \gg 1$. This limiting case corresponds to the classical electromagnetic field in the cavity. Let us represent the full Hamiltonian (6) as a sum of the "diagonal" part,

$$\hat{\mathcal{H}}_d = \hbar\omega_c a^\dagger a + \frac{\Delta}{2}\sigma_z + g_S(a + a^\dagger)(\sigma_z + I), \tag{19}$$

and the "off-diagonal" part,

$$\hat{\mathcal{H}}_{\rm od} = g_R(a\sigma^+ + a^\dagger\sigma^-). \tag{20}$$

The Hamiltonian (19) does not commute with the excitation number operator (10) but does commute with the Pauli matrix σ_z. This means that eigenstates of the Hamiltonian (19) can be represented as

$$\left|\psi_n^g\right\rangle = \sum_{k=0}^{\infty} C_{nk}^g|g,k\rangle, \tag{21}$$

$$\left|\psi_n^e\right\rangle = \sum_{k=0}^{\infty} C_{nk}^e|e,k\rangle. \tag{22}$$

After substituting the expressions (21) and (22) into the Schrödinger equation $\hat{\mathcal{H}}_d|\psi_n^{g,e}\rangle = \varepsilon_n^{g,e}|\psi_n^{g,e}\rangle$ with the Hamiltonian (19), we obtain the system of algebraic equations for

coefficients $C^{g,e}_{nk}$:

$$\left[\hbar\omega_c k - \Delta/2 - \varepsilon^g_n\right]C^g_{nk} = 0 \tag{23}$$

for $k = 0,1,2,\ldots,$

$$\left[\hbar\omega_c k + \Delta/2 - \varepsilon^e_n\right]C^e_{nk} + 2g_S\sqrt{k+1}C^e_{n,k+1} = 0 \tag{24}$$

for $k = 0,1,$

$$\left[\hbar\omega_c k + \Delta/2 - \varepsilon^e_n\right]C^e_{nk} + 2g_S(\sqrt{k+1}C^e_{n,k+1} + \sqrt{k}C^e_{n,k-1}) = 0 \tag{25}$$

for $k = 2,3,4,\ldots.$

The solutions of Eqs. (23) are evident,

$$\varepsilon^g_n = \hbar\omega_c n - \frac{\Delta}{2}, \quad C^g_{nk} = \delta_{nk}. \tag{26}$$

As for Eqs. (25), in the limiting case $k \gg 1$ they are similar to the well-known recurrent expression for the Bessel function of the first kind,

$$2m J_m(x) = x J_{m-1}(x) + x J_{m+1}(x), \tag{27}$$

where m is an integer and x is the argument of the Bessel function of the first kind, $J_m(x)$. Therefore, we can write the solutions of Eqs. (25) for $k \gg 1$ as

$$\varepsilon^e_n = \hbar\omega_c n + \frac{\Delta}{2}, \quad C^e_{nk} = J_{k-n}(x_k), \tag{28}$$

where $x_k = -4g_S\sqrt{k}/\hbar\omega_c$. It should be noted that the solutions (28) satisfy Eqs. (24) and (25) for small integers $k \sim 1$ as well, since

$$\lim_{n\to\pm\infty} J_n(x) = 0.$$

As a result, for large photon occupation numbers n the eigenfunctions (21) and (22) take the form

$$\left|\psi^g_n\right\rangle = |g,n\rangle, \tag{29}$$

$$\left|\psi^e_n\right\rangle = \sum_{k=0}^{\infty} J_{k-n}(x_k)|e,k\rangle. \tag{30}$$

Let us make n and V tend to infinity while keeping n/V constant. This limiting case corresponds to the conventional model of an intense laser-generated field [24]. Then $x_n = (\mathbf{d}_{ee}\cdot\mathbf{e})E_n/\hbar\omega_c$, where $E_n = \sqrt{2n\hbar\omega_c/\epsilon_0 V}$ is the classical amplitude of the field. Therefore, in the case of the most relevant physical situation with $x_n \ll 1$, the eigenfunctions (30) can be estimated as $|\psi^e_n\rangle \approx |e,n\rangle$ since $J_{k-n}(0) = \delta_{k,n}$. This allows us to seek eigenfunctions of the full Hamiltonian $\hat{\mathcal{H}} = \hat{\mathcal{H}}_d + \hat{\mathcal{H}}_{od}$ as a superposition (linear combination) of the functions (29) and (30). Substituting this superposition $\psi^{\pm}_n$ into the Schrödinger equation $\hat{\mathcal{H}}|\psi^{\pm}_n\rangle = \varepsilon^{\pm}_n|\psi^{\pm}_n\rangle$, we can find the energy spectrum $\varepsilon^{\pm}_n$ of the coupled electron-photon system. Particularly for the resonance case ($\Delta = \hbar\omega_c$), this linear combination is

$$|\psi^{\pm}_n\rangle = \frac{1}{\sqrt{2}}\left(\left|\psi^e_n\right\rangle \pm \left|\psi^g_{n+1}\right\rangle\right) \tag{31}$$

and the corresponding energies are

$$\varepsilon^{\pm}_n = \hbar\omega_c n + \varepsilon_e \pm \frac{\hbar\Omega'_R}{2}, \tag{32}$$

where $\Omega'_R = (\mathbf{d}_{eg}\cdot\mathbf{e})E_n/\hbar$ is the Rabi frequency for the classically strong electromagnetic field. It follows from the expressions (29)–(31) that the states with all possible numbers of excitations become intermixed. This means that all transitions $|\psi^{\pm}_n\rangle \to |\psi^{\pm}_m\rangle$ are allowed and emission spectrum contains frequencies $(n-m)\hbar\omega_c \pm \Omega'_R$. However, the intensity of the transitions decreases with increasing $(n-m)$ because of decreasing the Bessel functions $J_k(x)$ with increasing k [20]. Therefore, the most intensive ones correspond to those depicted in Fig. 2. This agrees with the results obtained above in the frameworks of perturbation theory for the weak asymmetry case.

It should be noted that there is no analytical solution for arbitrary photon occupation numbers of the cavity mode and arbitrary asymmetry strength. To study physically relevant situations outside the obtained analytical solutions as well as to calculate the shape of the emission spectrum, we need to apply the numerical approach discussed in the next section.

IV. NUMERICAL APPROACH

The discussion in the previous section was dedicated to the analytical calculation of the energy spectrum of the system. We were able to find the emission frequencies in two limiting cases corresponding to weak asymmetry and large photon occupation numbers. However, even in these cases, our treatment did not allow us to calculate the shape of the emission spectrum as a function of the intensity of the external pump. In this section we calculate it numerically using the approach based on the master equation techniques.

Let us assume that one has a QD embedded in a microcavity and switches on incoherent pumping of the photonic mode. After some time an equilibrium is established and steady state (SS) is reached. This means that the increase of photon number provided by external pumping is balanced by escape of photons from the cavity. In this regime, one can measure the emission spectrum, i.e., the intensity of the flux of the photons going out from the cavity as a function of their frequency.

In quantum optics, the standard way to consider the processes involving external pumping and decay is based on using the master equation for the full density matrix of the system ρ (see, e.g., Ref. [25]), which can be represented in the following form:

$$\partial_t\rho = \frac{1}{i\hbar}[\hat{\mathcal{H}};\rho] + \mathcal{L}\rho. \tag{33}$$

The first term on the right-hand side of the equation, $\hat{\mathcal{H}}$, stands for the Hamiltonian describing coherent processes in the system, and the symbol $\mathcal{L}$ denotes the Lindblad superoperator accounting for pump and decay. In the case we consider, $\hat{\mathcal{H}}$ is given by the expression (6), while the Lindblad term reads

$$\begin{aligned}\mathcal{L}\rho = {} & P(a\rho a^\dagger + a^\dagger\rho a - a^\dagger a\rho - \rho a a^\dagger) \\ & + \frac{\gamma_{\rm ph}}{2}(2a\rho a^\dagger - \rho a^\dagger a - a^\dagger a\rho) \\ & + \frac{\gamma_{\rm QD}}{2}(2\sigma\rho\sigma^+ - \rho\sigma^+\sigma - \sigma^+\sigma\rho).\end{aligned} \tag{34}$$

Here P is the intensity of the incoherent pump of the cavity mode and $\gamma_{\rm ph}$ and $\gamma_{\rm QD}$ are broadenings of photonic and excitonic modes, respectively (the latter is taken to be zero

in all calculations below). Equation (33) represents a set of linear ordinary differential equations for matrix elements of the density matrix ρ. In our numerical analysis we will use the basis

$$|g,n\rangle, |e,n\rangle, \tag{35}$$

which gives us the following system of equations, which can be written briefly as

$$\partial_t \rho_{ij}^{ab} = \sum_{k,l;c,d} M_{ijkl}^{abcd} \rho_{kl}^{cd}, \tag{36}$$

or, in the explicit form, as

$$\begin{aligned}\partial_t \rho_{ij}^{ab} &= \hbar\omega_c(i-j)\rho_{ij}^{ab} + \frac{\Delta}{2}[(-1)^{\delta_{ag}} - (-1)^{\delta_{bg}}]\rho_{ij}^{ab} + g_R\left(\sqrt{i+1}\delta_{ae}\rho_{i+1,j}^{ab} + \sqrt{i}\delta_{ag}\rho_{i-1,j}^{ab} - \sqrt{j}\delta_{bg}\rho_{i,j-1}^{ab} - \sqrt{j+1}\delta_{be}\rho_{i,j+1}^{ab}\right) \\ &+ g_S\left(\sqrt{i+1}\delta_{ae}\rho_{i+1,j}^{ab} + \sqrt{i}\delta_{ae}\rho_{i-1,j}^{ab} - \sqrt{j}\delta_{be}\rho_{i,j-1}^{ab} - \sqrt{j+1}\delta_{be}\rho_{i,j+1}^{ab}\right)2 \\ &+ \frac{P}{2}\left[2\sqrt{(i+1)(j+1)}\rho_{i+1,j+1}^{ab} + 2\sqrt{ij}\rho_{i-1,j-1}^{ab} - (2i+2j+2)\rho_{i,j}^{ab}\right] \\ &+ \frac{\gamma_{\rm ph}}{2}\left[2\sqrt{(i+1)(j+1)}\rho_{i+1,j+1}^{ab} - (i+j)\rho_{i,j}^{ab}\right] + \frac{\gamma_{\rm QD}}{2}\left(2\rho_{i,j}^{ab}\delta_{ag}\delta_{bg} - \rho_{i,j}^{ab}\delta_{ae} - \rho_{i,j}^{ab}\delta_{be}\right).\end{aligned} \tag{37}$$

Here the superscripts a,b,c,d are either g or e (ground or excited state of the QD) and the subscripts i,j,k,l correspond to the number of the photons in a cavity. In principle, they can take values from zero to infinity, but, for numerical analysis, truncation of the matrix is needed. The stronger the pump, the more states should be taken into account. The natural way to control the accuracy of the truncation is to check the conservation of the trace of the truncated density matrix.

A numerical solution of the system (36) allows us to find the full density matrix of the system in stationary state, $\rho_{ij}^{ab(SS)}$, which allows us to determine the probabilities of the occupancies of different quantum states of the coupled QD-cavity system as functions of the intensity of the external pump. As well, it allows us to find the shape of the emission spectrum of the system. To pursue this latter task, we will use the two approaches. Let us start with the relatively simple model based on the modified Fermi golden rule, considering the isolated QD-cavity system. Its eigenstates can be found by diagonalization of the Hamiltonian (6). This procedure was performed analytically in the previous section for the cases of weak asymmetry and large photonic occupation numbers. However, in the general case, a numerical analysis is needed. Let us suppose that we prepare a system in one of the eigenstates of the Hamiltonian. Then, according to the Fermi golden rule, we can estimate the emission spectrum as

$$\begin{aligned}S(\omega) &\sim \sum_{if} |\langle\psi_f,1_R|\hat{\mathcal{H}}_{\rm ex}|\psi_i,0_R\rangle|^2 \wp(\omega)\frac{\gamma_{\rm ph}^2}{(\varepsilon_f-\varepsilon_i-\hbar\omega)^2+\gamma_{\rm ph}^2} \\ &\sim |a_{if}|^2\wp(\omega)\frac{\gamma_{\rm ph}^2}{(\varepsilon_f-\varepsilon_i-\hbar\omega)^2+\gamma_{\rm ph}^2},\end{aligned} \tag{38}$$

where the symbols ψ_f,ψ_i denote the final and initial eigenstates of the Hamiltonian (6), 0_R and 1_R describe zero- and one-photon states of the reservoir, $\hat{\mathcal{H}}_{\rm ex}$ is the Hamiltonian of the coupling between the cavity and reservoir [see Eq. (12)], and $\wp(\omega)$ is the density of states in the reservoir, $a_{if} = \langle\psi_i|a|\psi_f\rangle$. The Lorentzian factor accounts for the broadening of the state, $\gamma_{\rm ph}$, provided by finite lifetime of cavity photons.

If the system is in the mixed state, the spectrum can be estimated as a sum over all possible initial states taken with corresponding probabilities P_i,

$$S(\omega) \sim \frac{2\pi}{\hbar}\sum_{if} P_i|a_{fi}|^2\wp(\omega)\frac{\gamma_{\rm ph}^2}{(\varepsilon_f-\varepsilon_i-\hbar\omega)^2+\gamma_{\rm ph}^2}. \tag{39}$$

Parameters P_i entering into the above expression are nothing but diagonal matrix elements of the density matrix in the stationary state written in the basis of eigenstates of the Hamiltonian (6), $P_i = \tilde{\rho}_{ii}^{SS}$. The matrix $\tilde{\rho}^{SS}$ can be found by a unitary transformation of the stationary density matrix in the basis $(|e,n\rangle, |g,n\rangle)$ obtained from solution of Eqs. (36).

The described phenomenological approach for calculating the emission spectrum has one substantial drawback, namely we assume the peaks in the spectrum to be Lorentzians, which is not always guaranteed [23,26,27]. In general, according to the Wiener-Khintchine theorem [28], the spectrum of the emission from the system can be calculated as a Fourier transform of two-time correlator,

$$S(\omega) \sim \lim_{t\to\infty}\mathcal{R}\int_0^\infty \langle a^\dagger(t+\tau)a(\tau)\rangle e^{i\omega\tau}d\tau. \tag{40}$$

The calculation of two-time correlators is a complicated task which cannot be solved exactly. However, it is well known from the literature [23,28] that using certain general assumptions about the behavior of the system allows one to reduce the calculation of two-time correlators to calculation of one-time correlators within the framework of the quantum regression theorem (QRT) [29]. This means that the spectrum can be calculated straightforwardly from the density matrix of the system in stationary state. For the system we consider in the present paper, the approach based in QRT results in

$$S(\omega) = \frac{1}{\pi}\mathcal{R}\sum_{i,j,k,l;a,b}[(M+i\hbar\omega I)^{-1}]_{ij,kl}^{a,b}\left(\rho_{km}^{ab(SS)}\right)a_{lm}a_{ji}, \tag{41}$$

where M is the matrix defined in Eqs. (36) and (37) and I is the unity matrix. It should be noted that the expression above is valid for any choice of the basis.

The shape of the emission spectrum of the system calculated using the Fermi golden rule and QRT is analyzed in the following section.

V. DISCUSSION

The emission spectrum of the system, calculated using the phenomenological approach based on the Fermi golden rule, is presented in Fig. 3.

One sees that in the region of the frequencies close to the eigenfrequency of the cavity (coinciding with the frequency of optical transition in QD, $\hbar\omega_c = \Delta$), the spectrum reveals a quadruplet pattern. The appearance of the additional multiplets is not visible in the linear scale but becomes apparent in logarithmic scale as shown in Fig. 4. These results are in good qualitative agreement with those obtained earlier for the symmetric QDs in the strong-coupling regime [14]. This is not surprising, since the main difference in the emission from the symmetric and asymmetric QDs appears at the regions around the Rabi frequency and the double frequency $2\omega_c$.

The insets in Figs. 3 and 4 show the emission pattern at the THz range about Ω_R. In full agreement with results of Sec. II, one sees the appearance of the peaks in the emission at frequencies $\omega = \Omega_R\sqrt{n}$ with $n = 1,2,3,\ldots$. It should be noted that one should expect very low intensities of THz emission as compared to the emission in the optical diapason, since density of states of the photon reservoir scales as ω^3. However, the situation can be improved if the coupled QD-cavity system is placed inside a bigger cavity tuned at the THz range. In this case, the density of states has a sharp peak around the eigenfrequency of the THz cavity and the rate of spontaneous emission is dramatically increased due to the Purcell effect [30]. The current state of technology allows us to increase the emission rates in the THz regime by a factor of 10 in high-quality cavities [31].

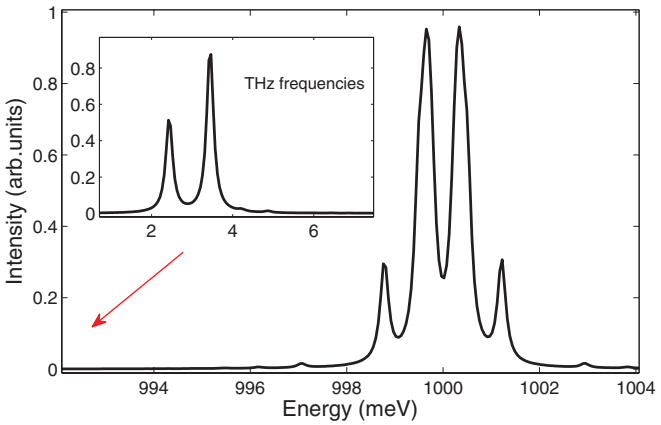

FIG. 3. (Color online) Emission spectrum of the asymmetric QD-cavity system calculated using the Fermi golden rule. The standard quadruplet structure is revealed in an optical diapason close to the eigenfrequency of the cavity. An additional set of emission peaks appears in the range of frequencies close to the Rabi frequency. They are provided by the asymmetry of the QD and are absent in a symmetric case. The parameters of the calculation are $\gamma_{\rm ph} = 0.1$ meV, $\gamma_{\rm QD} = 0$, $P \approx 0.15$ meV, $\hbar\omega_c = \Delta = 1$ eV, $g_R \approx g_S \approx 1$ meV.

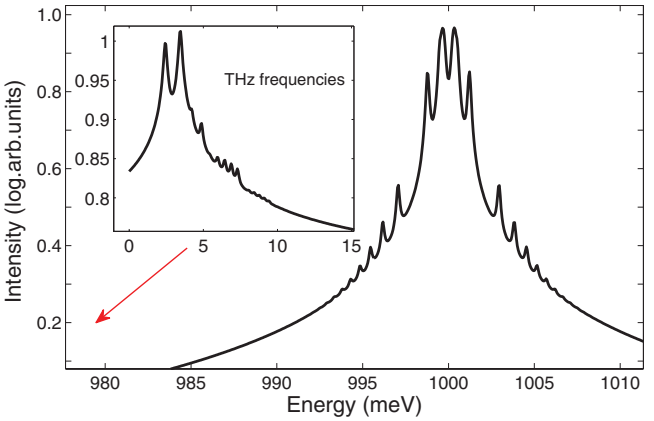

FIG. 4. (Color online) Emission spectrum of the asymmetric QD-cavity system calculated using the Fermi golden rule in a logarithmic scale. The multiplet structure of the emission around the eigenfrequency of the cavity becomes more visible than in the linear scale. An additional set of emission peaks appears in the range of the frequencies close to Rabi frequency. Parameters of the system are the same as for Fig. 3.

The results of the calculation of the spectrum based on using the quantum regression theorem are presented in Fig. 5. The part of the spectrum corresponding to the optical diapason for the frequencies about $\omega \approx \omega_c$ is in good agreement with results obtained by using the Fermi golden rule (Figs. 3 and 4). The differences are that the side peaks in the QRT plots have lower intensities, and the shape of the spectrum is more smooth, so the multiplet pattern becomes invisible.

The changes in the THz part are more dramatic. Instead of a series of narrow peaks, shown in the inset of Fig. 5, one sees a formation of a single broad strongly asymmetric peak centered at the frequency $\omega \approx \Omega_R$. However, the qualitative result remains the same: new optical transitions in the THz range are opened by the asymmetry of the QD.

The important question is in regard to statistical properties of the emitted THz light. As the emission spectrum we obtain is

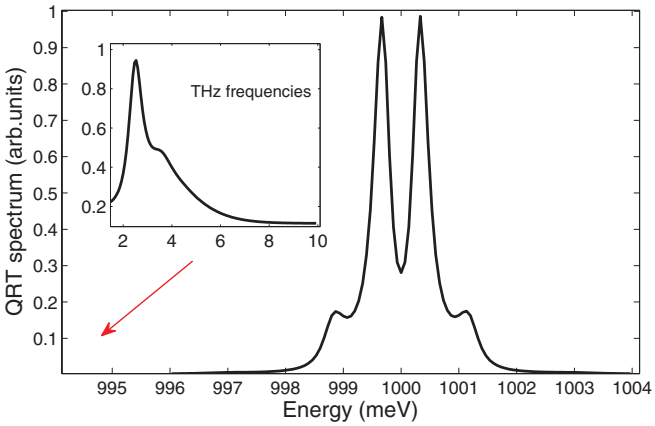

FIG. 5. (Color online) Emission spectrum of the asymmetric QD-cavity system calculated using QRT. The standard quadruplet structure is revealed in an optical diapason close to the eigenfrequency of the cavity. A single broad asymmetric emission peak appears in the range of the frequencies close to the Rabi frequency. The parameters of the calculation are the same as described in the caption to Fig. 3.

quite broad, and the efficiency of the THz emission is normally suppressed as compared to the emission at optical frequencies, one can expect that the emitted radiation will have thermal statistics with second-order coherence $g^{(2)} \approx 2$. On the other hand, placing the sample into a high-quality THz cavity can lead to the selection of a more narrow region of the frequencies of the emission. In this case, one can expect to achieve a THz lasing regime with $g^{(2)} \approx 1$. Detailed consideration of this situation, however, lies beyond the scope of the present paper. As to detection of the emitted THz radiation, it can be achieved by standard THz detectors (see, e.g., the review in Ref. [32]).

VI. CONCLUSIONS

In conclusion, we considered an asymmetric two-level quantum system corresponding to a small asymmetric QD interacting with an electric field of a single-mode microcavity. We found analytical solutions for the eigenenergies of the system for the cases of weak asymmetry and high photon occupation numbers. We also developed a numerical approach to calculate the emission spectrum under incoherent pumping. It is shown that, in the regime of a strong pump, a new set of peaks in the emission appears in the regions close to the Rabi frequency and double transition frequency. This allows one to use the proposed system as nonlinear optical element and tunable source of the THz radiation.

ACKNOWLEDGMENTS

The work was partially supported by Rannis "Center of excellence in polaritonics," the RFBR Project No. 10-02-00077, the Russian Ministry of Education and Science, the 7th European Framework Programme (Grants No. FP7-230778, No. FP7-246912, No. FP7-295187, and No. FP7-246784), and ISTC Project No. B-1708. We thank Dr. F. Laussy for useful discussions and the International Institute of Physics (Natal, Brazil) for hospitality.

[1] C. Weisbuch, M. Nishioka, A. Ishikawa, and Y. Arakawa, Phys. Rev. Lett. **69**, 3314 (1992).
[2] See, e.g., a special volume devoted to a physics of microcavities, Phys. Status Solidi B Vol. **242**, No. 11.
[3] J. Kasprzak, M. Richard, S. Kundermann, A. Baas, P. Jeambrun, J. M. J. Keeling, F. M. Marchetti, M. H. Szymanska, R. Andre, J. L. Staehli, V. Savona, P. B. Littlewood, B. Deveaud and Le Si Dang, Nature **443**, 409 (2006); R. Balili, V. Hartwell, D. Snoke, L. Pfeiffer, and K. West, Science **316**, 1007 (2007).
[4] I. Carusotto and C. Ciuti, Phys. Rev. Lett. **93**, 166401 (2004); I. A. Shelykh, Yu.G. Rubo, G. Malpuech, D. D. Solnyshkov, and A. V. Kavokin, *ibid*. **97**, 066402 (2006).
[5] I. A. Shelykh, K. V. Kavokin, A. V. Kavokin, G. Malpuech, P. Bigenwald, H. Deng, G. Weihs, and Y. Yamamoto, Phys. Rev. B **70**, 035320 (2004).
[6] S. Christopoulos, G. Baldassarri Hoger von Hogersthal, A. J. Grundy, P. G. Lagoudakis, A. V. Kavokin, J. J. Baumberg, G. Christmann, R. Butte, E. Feltin, J.-F. Carlin, and N. Grandjean, Phys. Rev. Lett. **98**, 126405 (2007).
[7] C. Leyder, T. C. H. Liew, A. V. Kavokin, I. A. Shelykh, M. Romanelli, J. Ph. Karr, E. Giacobino, and A. Bramati, Phys. Rev. Lett. **99**, 196402 (2007).
[8] S. Savasta, O. Di Stefano, V. Savona, and W. Langbein, Phys. Rev. Lett. **94**, 246401 (2005).
[9] C. Ciuti, Phys. Rev. B **69**, 245304 (2004); S. Savasta, O. Di Stefano, V. Savona, and W. Langbein, Phys. Rev. Lett. **94**, 246401 (2005).
[10] R. Johne, N. A. Gippius, G. Pavlovic, D. D. Solnyshkov, I. A. Shelykh, and G. Malpuech, Phys. Rev. Lett. **100**, 240404 (2008).
[11] J. P. Reithmaier, G. Sek, A. Loffler, C. Hofmann, S. Kuhn, S. Reitzenstein, L. V. Keldysh, V. D. Kulakovskii, T. L. Reinecker, and A. Forhel, Nature **432**, 197 (2004).
[12] T. Yoshie, A. Scherer, J. Heindrickson, G. Khitrova, H. M. Gibbs, G. Rupper, C. Ell, O. B. Shchekin, and P. G. Deppe, Nature **432**, 200 (2004).
[13] E. Peter, P. Senellart, D. Martrou, A. Lemaitre, J. Hours, J. M. Gerard, and J. Bloch, Phys. Rev. Lett. **95**, 067401 (2005); M. A. Kaliteevski, S. Brand, R. A. Abram, A. Kavokin, and Le Si Dang, Phys. Rev. B **75**, 233309 (2007).
[14] Elena del Valle, Fabrice P. Laussy, and Carlos Tejedor, Phys. Rev. B **79**, 235326 (2009).
[15] Fabrice P. Laussy, Elena del Valle, and Carlos Tejedor, Phys. Rev. B **79**, 235325 (2009).
[16] F. P. Laussy, M. M. Glazov, A. Kavokin, D. M. Whittaker, and G. Malpuech, Phys. Rev. B **73**, 115343 (2006).
[17] E. T. Jaynes and F. W. Cummings, Proc. IEEE **51**, 89 (1963).
[18] B. R. Mollow, Phys. Rev. **188**, 1969 (1969).
[19] E. del Valle and F. P. Laussy, Phys. Rev. A **84**, 043816 (2011).
[20] O. V. Kibis, G. Ya. Slepyan, S. A. Maksimenko, and A. Hoffmann, Phys. Rev. Lett. **102**, 023601 (2009).
[21] K. V. Kavokin, M. A. Kaliteevski, R. A. Abram, A. V. Kavokin, S. Sharkova, and I. A. Shelykh, Appl. Phys. Lett. **97**, 201111 (2010).
[22] I. G. Savenko, I. A. Shelykh, and M. A. Kaliteevski, Phys. Rev. Lett. **107**, 027401 (2011).
[23] M. O. Scully and M. S. Zubairy, *Quantum Optics* (University Press, Cambridge, 2001).
[24] C. Cohen-Tannoudji, J. Dupont-Roc, and G. Grynberg, *Atom-Photon Interactions: Basic Processes and Applications* (Wiley, Chichester, 1998).
[25] A. V. Kavokin, J.J. Baumberg, G. Malpuech, and F. P. Laussy, *Microcavities* (University Press, Oxford, 2007).
[26] F. P. Laussy, A. Laucht, E. del Valle, J. J. Finley, and J. M. Villas-Boas, Phys. Rev. B **84**, 195313 (2011).
[27] E. del Valle, F. P. Laussy, Phys. Rev. A **84**, 043816 (2011).
[28] H. Carmichael, *An Open System Approach to Quantum Optics* (Springer-Verlag, Berlin, 1993).
[29] S. Swain, J. Phys. A: Math. Gen. **14**, 2577 (1981).
[30] E. M. Purcell, Phys. Rev. **69**, 681 (1946).
[31] Y. Todorov, I. Sagnes, I. Abram, and C. Minot, Phys. Rev. Lett. **99**, 223603 (2007).
[32] F. Sizov and A. Rogalski, Prog. Quantum Electron. **34**, 278 (2010).